

# Differentiated Bronchiolar Epithelium in Alveolar Ducts of Rats Exposed to Ozone for 20 Months

Kent E. Pinkerton,<sup>\*,†</sup> Daryn E. Dodge,<sup>\*</sup>  
Jane Cederdahl-Demmler,<sup>†</sup> Viviana J. Wong,<sup>†</sup>  
Janice Peake,<sup>†</sup> Carole J. Haselton,<sup>\*</sup>  
Paul W. Mellick,<sup>‡</sup> Gurmukh Singh,<sup>§</sup> and  
Charles G. Plopper<sup>\*,†</sup>

From the Department of Veterinary Anatomy and Cell Biology<sup>\*</sup> and California Regional Primate Research Center,<sup>†</sup> School of Veterinary Medicine, University of California, Davis, California; Battelle, Pacific Northwest Laboratories,<sup>‡</sup> Richland, Washington; Department of Veterans Affairs Medical Center,<sup>§</sup> University of Pittsburgh,  
Pittsburgh, Pennsylvania

**The effects of exposure to 1.0 ppm of ozone for twenty months were studied in male Fischer 344 rats. Light microscopic, morphometric, and immunohistological approaches were used to determine the distribution and degree of differentiation of ciliated and nonciliated bronchiolar epithelial (Clara) cells lining alveolar ducts of the central acinus, a primary target of ozone-induced lung injury. Alveolar duct pathways extending beyond the level of the most proximal alveolar outpocketing of terminal bronchioles were isolated in longitudinal profile. The distance that ciliated and nonciliated bronchiolar epithelial (Clara) cells projected down each alveolar duct pathway was determined by placing concentric arcs radiating outward from a single reference point at the level of the first alveolar outpocketing. A high degree of heterogeneity in the magnitude of bronchiolar epithelial cell extension into alveolar ducts was noted for each isolation and animal. Age-matched control animals also demonstrated variation in the degree of bronchiolar epithelial cell extension down alveolar ducts. In animals exposed to ozone, a striking similarity was noted by scanning electron microscopy in the surface characteristics of cells lining both terminal bronchioles and alveolar ducts. The presence of Clara cell secretory protein in cells of bronchioles and alveolar ducts was also detected immunohistochemically and visualized using confocal laser scanning microscopy in the reflectance mode. Well-differentiated**

**ciliated and nonciliated bronchiolar epithelial cells were found lining alveolar septal tips and alveoli up to a depth of 1,000  $\mu$  into the pulmonary acinus after 20 months of exposure to ozone. No evidence of inflammation was present in alveolar ducts, suggesting that epithelial cell transformations in alveolar ducts is a natural consequence of lifetime exposures to oxidant gases. (Am J Pathol 1993, 142:947-956)**

The bronchiole-alveolar duct junction (BADJ) is one of the primary sites for injury in the lungs resulting from exposure to oxidant air pollutants. A number of studies have suggested that a major sequela of long-term, continuous exposure to oxidant gases is the reorganization of the epithelium in this region. In species with extensive respiratory bronchioles, such as primates, this reorganization involves extension of respiratory bronchiolar epithelium into more distal alveolar ducts.<sup>1,2</sup> In species with minimal respiratory bronchioles, such as the rat, chronic exposure is associated with the invasion of bronchiolar epithelium into alveolar ducts of the central acinus.<sup>3-6</sup> However, in the exposure time frames evaluated to date (90 days or less), characterization of epithelial populations as bronchiolar was based primarily on their cuboidal shape. These cells appear to be poorly differentiated, particularly at the more distal edges of their encroachment into alveolar ducts.<sup>3,4</sup> The purpose of the present study is to characterize the degree of differentiation of cuboidal epithelial cells lining distal air spaces in animals which had been exposed to ozone, an oxidant air pollutant, for the majority of their life span (20 months). The distribution of cuboidal epithelial cells along clearly defined alveolar duct paths and the degree of epithelial cell differentiation were evaluated. Cell differentiation was based on ciliated cells with well-defined cilia and nonciliated cells with apical surface protrusions

Accepted for publication September 10, 1992.

Address reprint requests to Dr. Kent E. Pinkerton, Department of Veterinary Anatomy and Cell Biology, University of California, Davis, CA 95616.

and containing Clara cell secretory product. In this study, alveolar duct paths were isolated in longitudinal profile from the BADJ and identified in all animals as beginning at the level of the first (most proximal) alveolar outpocketing of the terminal bronchiole.<sup>6</sup>

## **Materials and Methods**

### ***Animals and Exposure Conditions***

Exposure to ozone was performed at Battelle, Pacific Northwest Laboratories (Richland, WA) as part of a collaborative, multilevel study with the National Toxicology Program (NTP) and Health Effects Institute (HEI) to examine the long-term effects of ozone. Male Fischer 344 rats were obtained from Simonsen Laboratories (Gilroy, CA) at 4 to 5 weeks of age. Animals were randomly assigned to ozone exposure or control groups after a 10- to 14-day quarantine period. Animals were housed in modified Hazelton 2000 inhalation chambers and exposures were for 6 hours per day (between 7:30 a.m. and 5:30 p.m.), 5 days per week for 20 months. Due to the scope and number of animals required for the NTP/HEI study, the animals that formed the basis of this study were received from a total of 6 different exposure chambers (3 for ozone and 3 for filtered air). The average temperature range ( $\pm$ S.D.) within the exposure chambers over the course of the study was 23.9 to 24.4 ( $\pm$ 0.7) °C; the relative humidity range was 57.1 to 60.2 ( $\pm$ 7.3) percent.

Ozone was generated by corona discharge using an OREC Model 03V5-0 ozonator (Ozone Research and Equipment Corporation, Phoenix, AZ) with 100% oxygen. Ozone concentration in each chamber was monitored by a multiplexed Dasibi Model 1003-AH (Dasibi Environmental Corporation, Glendale, CA) ultraviolet spectrophotometric analyzer. Calibration of the monitor was accomplished by comparison with a chemical-specific calibrated (neutral buffered potassium iodide method) monitor simultaneously sampling the exposure chambers. The target concentration for ozone was 0.00 ppm for the control chambers and 1.00 ppm for the ozone chambers. The actual exposure concentration over the course of the study in the control chambers was less than 0.002 ppm (below the limit of detection) and 1.00 to 1.02 ( $\pm$ 0.07) ppm (mean  $\pm$  1 S.D.) in the ozone chambers. To determine concentration uniformity, measurements were periodically made at 12 levels or locations in each chamber. Ambient ozone was removed from all chambers using a potassium permanganate filter. Charcoal and HEPA filters were

used to further filter air entering the chambers. Following the end of the exposure, all animals were held for one week prior to sacrifice to emphasize permanent, nontransient changes in the lungs.

### ***Lung Fixation and Processing for Microscopy***

For this study, a total of four animals from the control group and four animals from the 1.0 ppm ozone exposure group were evaluated. Animals for analysis were selected by random number assignment.<sup>7</sup> The lungs were fixed by intratracheal instillation of 2% glutaraldehyde in cacodylate buffer (pH of 7.4, 350 mOsm).<sup>8,9</sup> In situ fixation of the lungs in the thorax was for 15 minutes at 30 cm fixative pressure. The lungs were collapsed by diaphragmatic puncture before fixative infusion. The fixed lungs were removed by thoracotomy and stored in the same fixative until processed for immunohistochemistry, histochemistry, light microscopy, and scanning electron microscopy. The fixed lungs were trimmed free of all mediastinal contents and the lung volumes measured by fluid displacement.<sup>10</sup> Six to eight regions were selected from the left lung lobe for complementary immunohistochemistry, histochemistry, and embedding for high resolution light microscopy.<sup>11</sup>

### ***Immunohistochemistry and Histochemistry***

Portions of the left lung were embedded in glycol methacrylate. One  $\mu$  sections were cut with glass knives on a JB4 microtome. Serial and serial-step sections were stained either with periodic acid Schiff and Alcian blue (pH 2.5)<sup>12,13</sup> or for Clara cell secretory protein (CCSP) with immunoperoxidase. For immunohistochemistry, the primary antibody, raised in rabbits against rat Clara cell secretory protein,<sup>14</sup> was followed by localization with avidin biotin peroxidase. The avidin biotin peroxidase reagents were obtained from Vector Laboratories, (Burlingame, CA) and used as recommended by the supplier with minor modifications.<sup>15</sup> The distribution of the reaction product was identified on 1  $\mu$  sections using a scanning laser confocal microscope (Biorad, Watford, England) in the reflectance mode. Methods controls included substitution of the primary antibody with normal rabbit serum.

### ***Scanning Electron Microscopy***

For scanning electron microscopy, the distal third of the right middle lobe was critical-point dried using

ethanol and carbon dioxide.<sup>16,17</sup> The distal conducting airways and the BADJs were identified by microdissection of critical-point-dried specimens.<sup>11</sup> The dissected lungs were mounted on stubs sputter-coated with gold and examined with a Phillips 501 microscope.

### *Bronchiole-Alveolar Duct Isolations for Light Microscopy*

Tissue slices cranial and caudal to the hilar level of the left lobe were embedded as large blocks for isolation of centriacinar regions by the methods of Pinkerton et al.<sup>6</sup> Briefly, tissue slices (approximately  $2 \times 4 \times 6$  mm in size) were post-fixed in 1% osmium tetroxide in Zetterquist's buffer, followed sequentially by 1% tannic acid and 1% uranyl acetate in maleate buffer, dehydrated in ethanol and propylene oxide and embedded in either Epon 812 or Araldite 502. Centriacinar regions were isolated by cutting the entire tissue block into slices approximately 0.3 to 0.4 mm thick. Each slice was examined under a dissecting microscope to identify BADJs in longitudinal profile. Criteria for selection was a symmetrical pair of alveolar ducts arising from a single terminal bronchiole. Isolations meeting this selection criteria consistently contained alveolar duct paths in longitudinal profile that extended two to four generations beyond the BADJ. Selected isolations were remounted on BEEM capsules and sectioned at a thickness of  $0.5 \mu$  with glass knives. Sections were stained with toluidine blue (0.5% in 1% borate buffer).

### *Quantitative Microscopy*

To measure the extent of differentiated bronchiolar epithelium into alveolar ducts, a rigid sampling scheme was employed.<sup>6</sup> Because rearrangement of the BADJ is a feature of chronic exposure to ozone, the distal end of the terminal bronchiole was identified based on locating the most proximal alveolar outpocketing in the airway wall (Figure 1). At the level of the proximal border of the first alveolar outpocketing, a reference point was placed in the geometric center of the airway lumen (Figure 1). From this reference point, a pattern of concentric circles at  $100 \mu$  intervals was drawn. Overlaying the concentric circle pattern onto each BADJ isolation was facilitated through the use of a Macintosh IIfx computer interfaced to an Olympus BH-2 microscope via a Dage MTI video camera (Michigan City, IN). The bull's eye pattern of concentric circles (set at  $100 \mu$  intervals

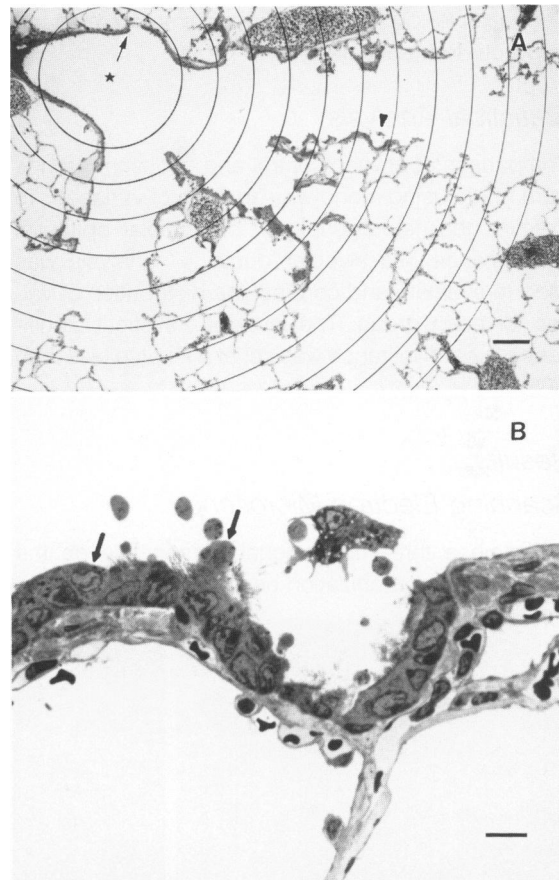


**Figure 1.** Profile of the BADJ and centriacinar region isolated from the lungs of a rat exposed to ozone for 20 months. The concentric arc pattern radiating from a reference point placed at the geometric center (star) of the bronchiole at the level of the first alveolar outpocketing is superimposed over the isolation. **B** is a higher magnification view of the area in **A** marked by the arrowhead. It shows the presence of ciliated cells (arrows) and nonciliated cells (arrowheads) with apical protrusions on septal tips and walls of the alveolar duct. (**A**: scale bar =  $100 \mu$ ; **B**: scale bar =  $10 \mu$ ).

relative to the resolution used) was stored as a computer file and could be directly overlaid and oriented over the captured computerized image of each isolation. Using a high resolution objective lens ( $\times 60$ ), the most distal extent of the most distal ciliated and nonciliated bronchiolar cells down each alveolar duct path was identified. Figure 1 illustrates the organization of this concentric circle overlay. The extent of cell extension down alveolar duct paths was determined using the concentric arc pattern as a measure of distance from a single reference point. If the distance that bronchiolar epithelial cells extended into the alveolar duct was less than  $200 \mu$ , the actual distance was measured from a distance perpendicular to the most proximal edge of the first alveolar outpocketing (arrow, Figure 1). A total of

eight alveolar duct isolations per animal were examined from four animals in each group.

### Statistical Analysis

Comparisons between control and exposure groups were made using a one-way analysis of variance. To examine the heterogeneity of bronchiolar epithelial cell distance into alveolar ducts,  $\chi^2$  analysis was used to evaluate and contrast the distribution of values for each group. The level of statistical significance in each instance was set at a *P* value less than 0.05.<sup>7</sup>

## Results

### Scanning Electron Microscopy

To obtain a three-dimensional perspective on the centriacinar reorganization occurring with long-term

ozone exposure, scanning electron microscopy was performed on complementary halves of BADJs. As illustrated in Figure 2, using the tilt function on the scanning electron microscope, it was possible to view all sides of the walls in this region. In animals exposed to air (Figure 2A,B) and to ozone (Figure 2C,D,E), the most proximal alveolar outpocketings were within 100  $\mu$  of the BADJ. In both control and ozone-exposed animals, the epithelial surface of the airway proximal to the first alveolar outpocketing was a mixture of ciliated cells and nonciliated cells, most of which had apical projections into the airway lumen. In control animals, the surface pattern of epithelial cells characteristic of those found in the terminal bronchiole was observed to extend to a variable distance beyond the most proximal alveolar outpocketing. This variation was observed from animal to animal, and from BADJ to BADJ within the same animal. Bronchiolar epithelial cells identified

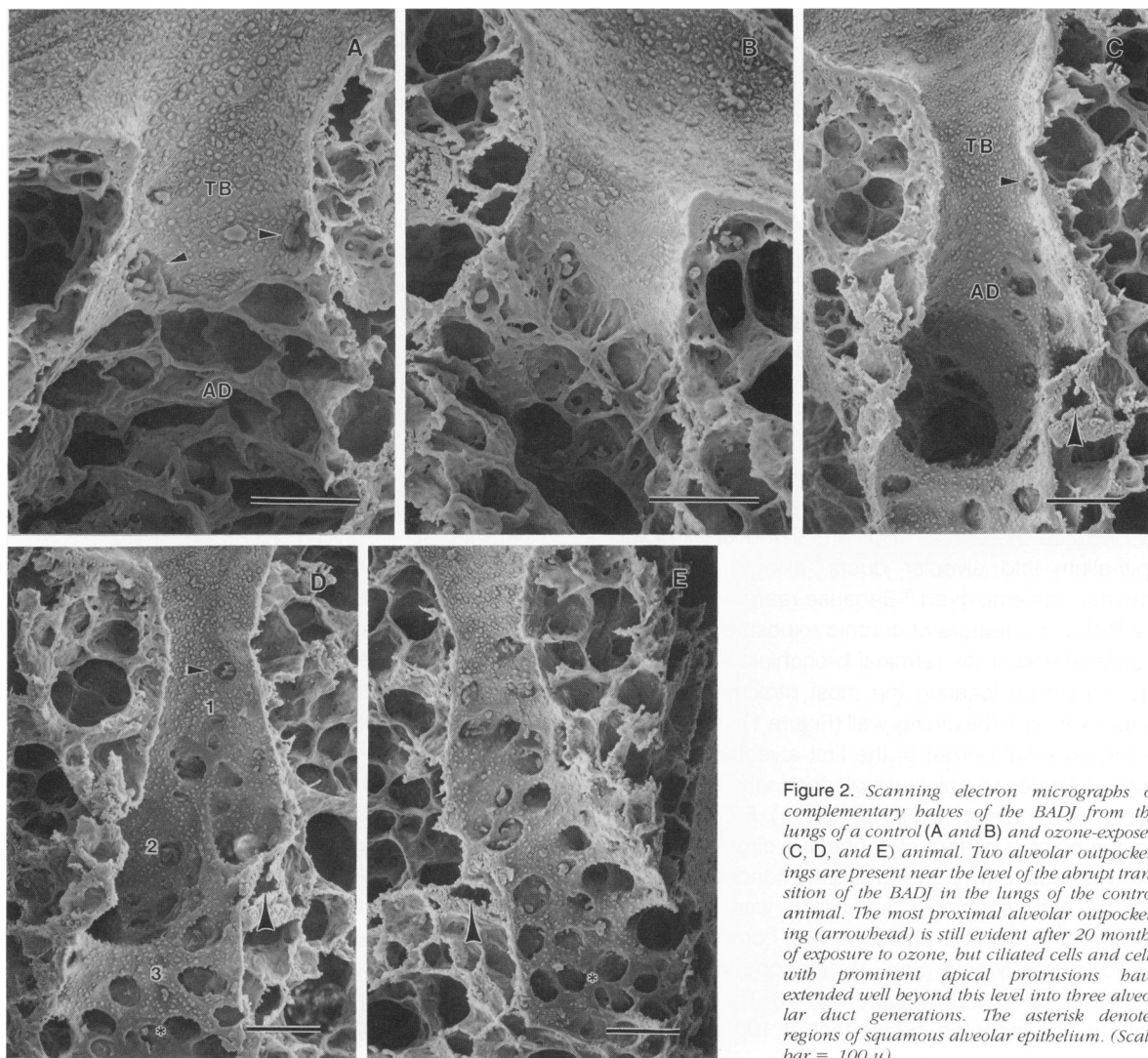


**Figure 2.** Scanning electron micrographs of complementary halves of the BADJ from the lungs of a control (A and B) and ozone-exposed (C, D, and E) animal. Two alveolar outpocketings are present near the level of the abrupt transition of the BADJ in the lungs of the control animal. The most proximal alveolar outpocketing (arrowhead) is still evident after 20 months of exposure to ozone, but ciliated cells and cells with prominent apical protrusions have extended well beyond this level into three alveolar duct generations. The asterisk denotes regions of squamous alveolar epithelium. (Scale bar = 100  $\mu$ ).

by their surface features, were occasionally found as far distally as the first bifurcation point of the alveolar duct. In animals exposed to ozone, the three-dimensional perspective on all portions of the airway wall indicated that the bronchiolar epithelium extended a number of generations into the alveolar ducts well beyond the first alveolar duct bifurcation ridge (Figure 2C,D,E). The surface characteristics of these cells within alveolar ducts appeared to be similar to those cells of the terminal bronchiole, although occasionally small regions within some alveolar duct generations contained squamous epithelial cells on the surfaces of alveolar mouth openings as well as in the alveolar outpockets (Figure 2D). The extent of bronchiolarization varied from animal to animal and from BADJ to BADJ. However, the surface pattern of bronchiolar epithelial cell types was relatively equal in extent around the entire circumference of affected alveolar ducts. Polarization of the bronchiolar epithelium in relation to the position of the pulmonary arteriole or the number of generations of branching of alveolar ducts in which the epithelium was observed was not apparent. In both control and exposed animals, where cuboidal cells with apical projections were observed in groups, ciliated cells were also present.

### *Immunohistochemistry of CCSP*

As a marker of the differentiation status of the cuboidal cells which we observed by scanning electron microscopy, we used the presence of antigen for CCSP. In control animals, the reaction product specific for CCSP was detectable in almost all of the nonciliated cells lining terminal bronchioles. The distribution of the product was clearly discernible by reflected light on 1  $\mu$  sections (Figure 3). The distribution of the ciliated and nonciliated cells on the same section could be characterized using DIC Nomarsky optics (Figure 3A). In BADJs where bronchiolar epithelium was present on the bifurcation ridge, as illustrated in Figure 3, CCSP could be detected in the nonciliated cells in this cuboidal epithelium (Figure 3B). At high magnification (Figure 3E,F), the distribution of ciliated cells and their relationship to nonciliated cells was detectable. The reaction product for CCSP was distributed most heavily in secretory granules but could also be observed in a reticulated pattern throughout the cell cytoplasm, with the exception of the nucleus. In exposed animals, the reaction product for CCSP was detectable in numerous generations of alveolar ducts (Figure 3C,D). All of the cuboidal epithelium we identified in alveolar ducts as being bronchiolar epithelium by morpho-

logical criteria contained nonciliated cells with a positive reaction for CCSP.

### *Distribution and Extent of Ciliated and Nonciliated Cells*

In toluidine blue-stained, 1  $\mu$  sections, the bronchiolar epithelium was characterized by its dense staining pattern (Figure 1). The heterogeneity in extent of bronchiolar epithelium into alveolar ducts was also discernible. As illustrated in Figure 1, bronchiolar epithelium occupied a variable extent of the alveolar ducts down different pathways in the same pulmonary acinus. At higher magnification, the densely staining epithelium in these distal regions contained cuboidal cells with identifiable cilia and nonciliated cells with apical projections (Figure 1B). Using these criteria, we observed a significant difference in the average distance ciliated and nonciliated (Clara) cells extended into alveolar ducts. In control animals, ciliated cells were found an average of 106  $\mu$  ( $\pm 23$ ) into the alveolar duct (Figure 4). In contrast, ciliated cells in exposed animals extended an average of 4 times deeper (476  $\mu \pm 34$ ) into the alveolar ducts compared to age-matched controls.

The heterogeneity of distribution for ciliated cells within alveolar ducts of control animals and animals exposed to ozone, is illustrated in Figure 5. For control animals, approximately half of the isolated alveolar duct paths had no ciliated cells distal to the most proximal alveolus. In 30% of alveolar ducts, ciliated cells were found between 20 and 200  $\mu$  distal to the most proximal alveolus. In less than 30% of alveolar duct paths, ciliated cells were observed more than 200  $\mu$  distal. In contrast, for animals exposed to ozone, every alveolar duct examined contained ciliated cells that extended beyond the most proximal alveolus. In over 35% of the alveolar duct paths, ciliated cells extended between 200 and 400  $\mu$  into the duct. In almost 50% of the alveolar duct paths in exposed animals, ciliated cells were found more than 400  $\mu$  from the most proximal alveolus. In almost 10% of the isolations, ciliated cells were found 800  $\mu$  or more into the acinus.  $\chi^2$  analysis confirmed a significant alteration in the relative distribution of ciliated cell distribution down alveolar duct paths in exposed animals compared with control animals.

Clara cells in control animals extended slightly further down alveolar duct paths (122  $\mu \pm 23$ ) than did ciliated cells (Figure 4). In animals exposed to ozone, Clara cells were observed 4 times deeper down alveolar duct paths (481  $\mu \pm 34$ ) compared to that observed in control animals (Figure 4). Almost 50% of the alveolar duct paths in control animals had

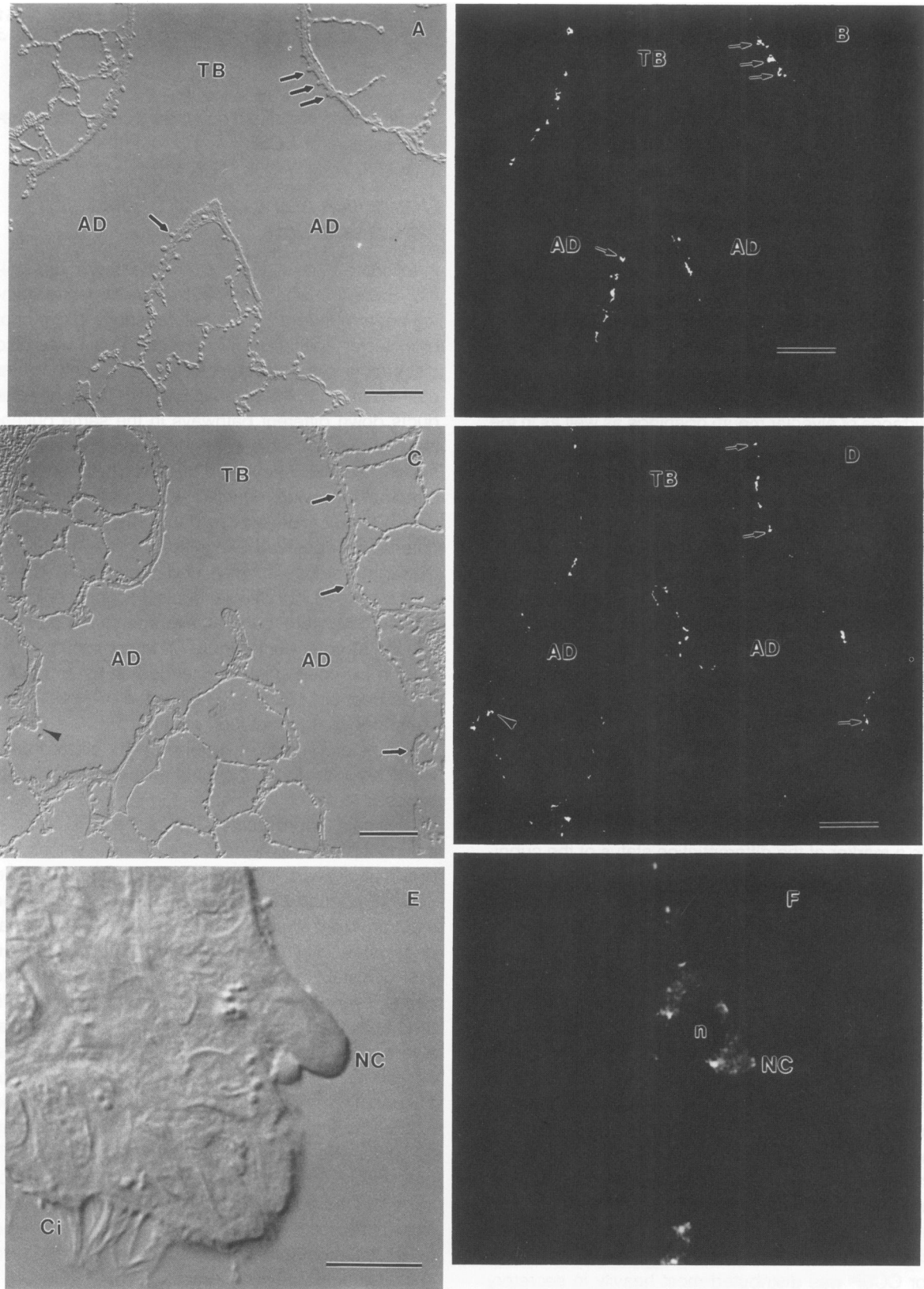


**Figure 3.** **A:** Terminal airway (DIC Normarsky optics). Apical domes of Clara cells (arrows) from a control rat lung are identifiable in epithelium lining terminal bronchioles (TB). There is an abrupt transition from bronchiole to alveolar duct (AD). (Scale bar = 100  $\mu$ ). **B:** Laser scanning confocal microscope image in the reflectance mode of same specimen as **A** shows the presence of CCSP in the Clara cells (arrows). No protein is detected in ciliated cells or in alveolar cells. (Scale bar = 100  $\mu$ ). **C:** Terminal airway from exposed rat (DIC Normarsky optics) showing extent of bronchiolar epithelium into alveolar ducts. Clara cell apical domes (arrows) are present in terminal bronchioles (TB) and in alveolar ducts (AD). (Scale bar = 100  $\mu$ ). **D:** Laser scanning confocal microscope image of same specimen as **C** shows the presence of CCSP in Clara cells (arrows) in both terminal bronchiole (TB) and alveolar duct (AD) zones. (Scale bar = 100  $\mu$ ). **E:** Higher magnification of Clara (NC) and ciliated (Ci) cells in epithelial lining of a respiratory bronchiole taken from the position in **C** and **D** marked by the arrowhead. CCSP is detectable in cells identified as Clara cells. Ciliated cells appear to have no product. (Scale bar = 10  $\mu$ ). **F:** Laser scanning confocal microscope image of same specimen as **E** shows the presence of CCSP in Clara cells but not in ciliated cells. Diaminobenzidine reaction product distributed most heavily in the granules. Nucleus (n) contained no reaction product. (Scale bar = 10  $\mu$ ).

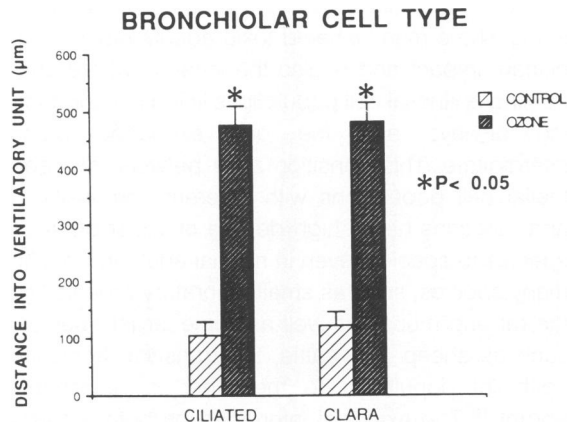


**Figure 4.** Bar graph summarizing the average distance (mean  $\pm$  S.E.M.) into alveolar ducts of ciliated and nonciliated bronchiolar epithelial (Clara) cells.

Clara cells that extended less than 20  $\mu$  into the pathway (Figure 6). The variation in extent of Clara cells in different alveolar ducts was similar for both Clara and ciliated cells in control animals (compare Figures 5A and 6A). In none of the alveolar ducts in exposed animals were Clara cells found less than 20  $\mu$  from the most proximal alveolar outpocket. The heterogeneity in the extent of Clara cell distribution down alveolar duct pathways was similar to that observed for ciliated cells (compare Figures 6B with 5B). As with ciliated cells, the extent of Clara cell distribution into alveolar ducts was significantly different between control and exposed animals by  $\chi^2$  analysis.

## Discussion

The reorganization of the centriacinar regions of the lung is a well-recognized result of continued inhalation of toxic oxidant gases at high ambient levels. Previous work from our group and others has shown that reasonably long-term (2-to-3-month) exposure to oxidant air pollutants, such as ozone and nitrogen dioxide, alters the mixture of epithelial cell populations occupying the proximal gas exchange areas of pulmonary acini in species with short or nonexistent respiratory bronchioles.<sup>3-18</sup> The present study addresses some of the questions raised by these previous investigations. What is the extent of the reorganized proximal alveolar ducts? How heterogeneous is the extent of this reorganization within the centriacinar regions of the same animal or between animals? What is the degree of differentiation of the bronchiolar epithelium that becomes associated with alveolar gas exchange areas? Does extended exposure, up to essentially a lifetime, alter the degree of reorganization?

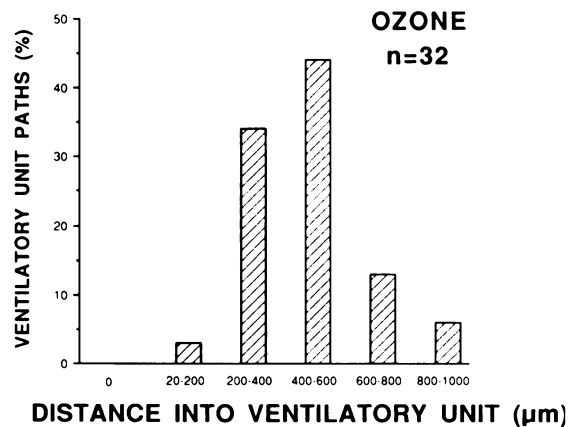
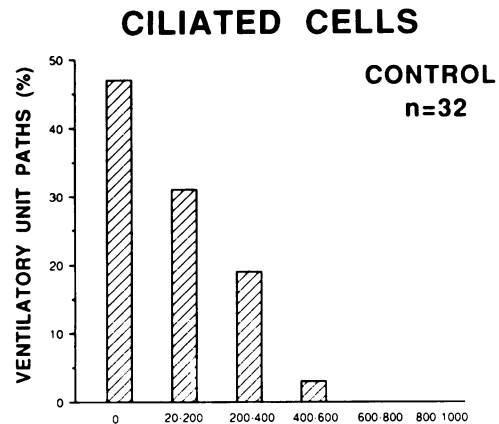


**Figure 5.** Distribution of differences in maximum extent of ciliated cells down alveolar duct paths. Class sizes are 0 to 19.9  $\mu$ , 20 to 199.9  $\mu$ , 200 to 399.9  $\mu$ , 400 to 599.9  $\mu$ , 600 to 799.9  $\mu$ , and 800 to 999.9  $\mu$ . Each bar represents the percentage of the total alveolar duct paths evaluated.

Our study has shown that BADJ reorganization can extend for as many as five generations of branching into the pulmonary acinus. The remodeling is not polarized and involves all sides of an alveolar duct branch. The alterations in epithelial populations occur not only on the epithelial surfaces lining the alveolar duct lumen but also extend down into alveolar outpocketings. We have also observed extensive heterogeneity in the degree of remodeling. This occurs even in different alveolar duct pathways arising from the same terminal bronchiole (Figure 1). In the control animals of this study, we also found the presence of bronchiolar epithelium into alveolar duct branches to varying degrees. In some cases, bronchiolar epithelium was present on a wall of an alveolar duct that also contained gas exchange regions. In other cases, there was a clear demarcation of the junction between the terminal bronchiole and first alveolar duct generation. Based on the structural

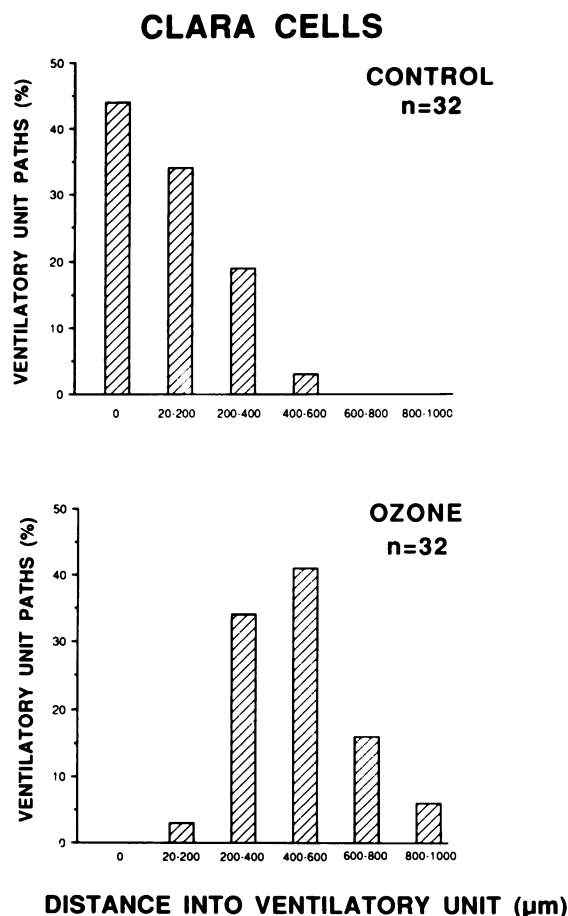


**Figure 6.** Distribution of differences in maximum extent of ciliated cells down alveolar duct paths. Class sizes are 0 to 19.9  $\mu$ , 20 to 199.9  $\mu$ , 200 to 399.9  $\mu$ , 400 to 599.9  $\mu$ , 600 to 799.9  $\mu$ , and 800 to 999.9  $\mu$ . Each bar represents the percentage of the total alveolar duct paths evaluated.

markers we used to gauge differentiation, the presence of extensive cilia or apical projections on cuboidal epithelial cells and the presence of Clara cell secretory protein, which appears to be unique to the secretory cells of terminal bronchioles in control animals, we concluded that the cuboidal populations lining the reorganized alveolar duct units express critical differentiated functions observed in terminal bronchiolar epithelial populations in unexposed animals. When our findings in this study are compared with previous studies, it seems that the inhalation of toxic oxidant gases over essentially a lifetime (i.e., 20 months) does not mitigate the extent or the nature of the remodeling that occurs with a shorter (2-to-3-month) exposure to ozone. In fact, our findings suggest that with repetitive exposure up to 20 months, the epithelial cell populations in remodeled airways achieve a higher degree of differentiated function than is observed with shorter (2-to-3-month) exposures.<sup>3-5</sup>

The centriacinar region is a prominent site in the lungs where many inhaled toxic agents have a significant impact and is also the location where contrasting epithelial cell populations lining the conducting airways and the gas exchange areas interdigitate. This transition zone between two epithelial cell populations with different compositions and functions has a high degree of variability from species to species, even in normal adult animals. In many species, such as small laboratory rodents like the rat and mouse as well as some larger species, such as sheep and cattle, the transition from one epithelial population to the other is reasonably abrupt.<sup>19</sup> The extent of interdigitation between epithelial populations that express differentiated functions characteristic of epithelium in more proximal airways into airway generations with epithelium characteristic of gas exchange areas is minimized and generally occurs at the branch point between airway generations or within the extent of one airway generation. In a large number of other species, including primates and most carnivores, this interdigitation and interaction is extensive and can include the epithelial lining of a large number of airway generations containing extensive areas of alveolar outpocketings. Therefore, in these regions a mixed population of bronchiolar and alveolar epithelial cells coexist. The response of this critical region to ozone may be different in humans and primates than in rodents. It is known that the epithelial cell composition of respiratory bronchioles in nonhuman primates can be significantly altered by exposure to ozone, with the extension of bronchiolar epithelium into alveolar ducts and an increase in the surface of respiratory bronchioles covered by nonalveolar epithelial cells.<sup>2</sup>

When the gas exchange area of rodent lungs is evaluated based on ventilatory units as described by Mercer and colleagues,<sup>20-22</sup> the heterogeneity in the extent of bronchiolar cell extension down alveolar duct paths becomes more apparent. A ventilatory unit of the lungs is defined as all alveolar ducts and alveoli extending from an airway branch in which the transition from bronchiolar epithelium to alveolar epithelium occurs.<sup>6,21,22</sup> Due to the extensive remodeling of the most proximal alveolar ducts arising from the terminal bronchiole, identification of the most proximal alveolar outpocketing along an airway was used as our point of reference to define the beginning of the ventilatory unit in rats. Mercer and coworkers have demonstrated that ventilatory unit volume in the lungs of rats is highly heterogeneous.<sup>20-22</sup> Ventilatory unit size has a significant impact on the volume of toxic gas that will pass

through the BADJ of that anatomical unit during an exposure. The heterogeneity and degree of bronchiolar cell extension down alveolar duct paths observed could be explained as a direct relationship to the dose of ozone and amount of injury occurring in this location. Whether this is the case cannot be determined from our study. However, the existence of ventilatory units with widely varying degrees of bronchiolarization, when combined with previous observations that ventilatory unit size can vary in volume by a factor of 3 to 10,<sup>22</sup> would suggest that this may be a major factor. What our study emphasizes is the need to explore more thoroughly the impact that ventilatory unit size can have on the response of epithelial populations within the target zone to oxidant air pollutants.

Transformation in the epithelial populations lining proximal alveolar ducts resulting from exposure to oxidant gases has been observed under a wide variety of exposure conditions. Proliferation and hyperplasia of cuboidal epithelial cells in zones previously occupied by squamous, alveolar type I cells occur as little as three days following initiation of exposure.<sup>23</sup> With extended exposures of up to three months, this population seems to be altered from what would be expected for a hyperplastic population of alveolar type II cells.<sup>3,24</sup> To the best of our knowledge, this is the first study that has addressed directly the extent of this epithelial transformation within the target zone. We have observed that this cuboidal population extends as much as 1,000  $\mu$  down into the gas exchange area following long-term exposure. We have also demonstrated that the extent is highly variable. Using the criteria for differentiation that we have applied would suggest that the longer the duration of exposure, the more differentiated this epithelial population will become. We base this primarily on the observation that we found cells with full length cilia well into alveolar duct regions. Previous studies have not clearly demonstrated the presence of well-ciliated cells in bronchiolar populations lining the target zone in animals exposed for shorter periods of time to approximately the same concentration.<sup>3,18</sup> Using another marker of differentiation, the presence of a secretory protein, our findings suggest that the nonciliated cells occupying these cuboidal populations in distal alveolar ducts are reasonably well-differentiated. Whether this is the case for shorter term exposures has not been evaluated.

The fact that bronchiolar epithelial cells can maintain a differentiated state over a long period of time in a zone where unexposed animals would have a completely different population mix opens a number of

questions concerning the regulation of differentiation and the control of epithelial population homeostasis in the respiratory system. The presence of epithelial cells expressing differentiated functions normally expressed by this population in a different zone suggests that multiple factors in the local microenvironment must be altered to produce this type of differentiation. Some of the factors in the local microenvironment that could be explored include changes in the interactions between interstitial cells and the epithelial population, alterations in the extracellular matrix, including composition of the basal lamina, and changes in mediators such as cytokines, which regulate epithelial functions in inflammatory responses.

### Acknowledgments

Research described in this article is conducted under contract to the Health Effects Institute (HEI), an organization jointly funded by the United States Environmental Protection Agency (Assistance Agreement X-816285) and automotive manufacturers. The contents of this article do not necessarily reflect the view of HEI nor do they necessarily reflect the policies of Environmental Protection Agency or automotive manufacturers. Animals were exposed as part of a National Toxicology Program (NTP)/HEI Collaborative Effort. The exposures were done at Battelle, Pacific Northwest Laboratories, under contract to NTP. The authors are appreciative of the coordination and planning efforts of Dr. Debra A. Kaden of HEI and Dr. Gary A. Boorman of NTP during the course of this study. This work was also supported in part by NIEHS grants ES00628 and ES04338.

### References

1. Castleman WL, Dungworth DL, Schwartz LW, Tyler WS: Acute respiratory bronchiolitis: an ultrastructural and autoradiographical study of epithelial cell injury and renewal in Rhesus monkeys exposed to ozone. *Am J Pathol* 1980, 98:811-827
2. Fujinaka LE, Hyde DM, Plopper CG, Tyler WS, Dungworth DL, Lollini LO: Respiratory bronchiolitis following long-term ozone exposure in bonnet monkeys: a morphometric study. *Exp Lung Res* 1985, 8:167-190
3. Barr BC, Hyde DM, Plopper CG, Dungworth DL: Distal airway remodeling in rats chronically exposed to ozone. *Am Rev Respir Dis* 1988, 137:924-938
4. Barr BC, Hyde DM, Plopper CG, Dungworth DL: A comparison of terminal airway remodeling in chronic daily versus episodic ozone exposure. *Toxicol Appl Pharmacol* 1990, 106:384-407

5. Boorman GA, Schwartz LW, Dungworth DL: Pulmonary effects of prolonged ozone insult in rats: morphometric evaluation of the central acinus. *Lab Invest* 1980, 43:108-115
6. Pinkerton KE, Mercer RR, Plopper CG, Crapo JD: Microdosimetry and microtoxicology of ozone in the ventilatory unit of the rat. *J Appl Physiol* 1992, 73:817-824.
7. Snedecor GW, Cochran WG: *Statistical Methods*, 6th ed. Ames, Iowa State University Press, 1967
8. Mori K: Induction of pulmonary tumors in rats by subcutaneous injections of 4-nitroquinoline 1-oxide. *Jpn J Cancer Res* 1962, 53:303-308
9. Dungworth DL, Tyler WS, Plopper CG: Morphologic methods for gross and microscopic pathology. *Toxicology of Inhaled Materials*. Edited by Witschi HP, Brain JD, New York, Springer-Verlag, 1985, pp 229-258
10. Scherle WF: A simple method of volumetry of organs in quantitative stereology. *Mikroskopie* 1970, 26:57-60
11. Plopper CG: Structural methods for studying bronchiolar epithelial cells. *Models of Lung Disease: Microscopy and Structural Methods*. Edited by Gil J, New York, Marcel Dekker, 1990, pp 537-559
12. Plopper CG, Heidsiek JG, Weir AJ, St. George JA, Hyde DM: Tracheobronchial epithelium in the adult rhesus monkey: a quantitative histochemical and ultrastructural study. *Am J Anat* 1989, 184:31-40
13. St. George JA, Plopper CG, Etchison JR, Dungworth DL: An immunocytochemical/histochemical approach to tracheobronchial mucus characterization in the rabbit. *Am Rev Respir Dis* 1984, 130:124-127
14. Singh G, Katyal SL: An immunologic study of the secretory products of rat Clara cells. *J Histochem Cytochem* 1984, 32:49-54
15. St. George JA, Cranz DL, Zicker S, Etchison JR, Dungworth DL, Plopper CG: An immunohistochemical characterization of rhesus monkey respiratory secretions using monoclonal antibodies. *Am Rev Respir Dis* 1985, 132:556-563
16. Tyler WS, Dungworth DL, Plopper CG, Hyde DM, Tyler NK: Structural evaluation of the respiratory system. *Fundam Appl Toxicol* 1985, 5:405-422
17. Karrer HE: The fine structure of connective tissue in the Tunica Propria of bronchioles. *J Ultrastruc Res* 1958, 2:96-121
18. Boorman GA, Schwartz LW, Dungworth DL: Pulmonary effects of prolonged ozone insult in rats: morphometric evaluation of the central acinus. *Lab Invest* 1980, 43:108-115
19. Plopper CG, Hyde DM, Buckpitt AR: Clara cells. *The Lung: Scientific Foundations*. Edited by Crystal RG, West JB, New York, Raven Press, Ltd., 1991, pp 215-226
20. Mercer RR, Crapo JD: Three-dimensional reconstruction of the rat acinus. *J Appl Physiol* 1987, 63:785-794
21. Mercer RR, Pinkerton KE: The influence of ventilatory unit size on the distribution and uptake of reactive gases. *Biofluid Mechanics*, vol. 3. Edited by Schneck DJ, Lucas CL, New York, New York University Press, 1990, pp 27-35
22. Mercer RR, Anjilvel S, Miller FJ, Crapo JD: Inhomogeneity of ventilatory unit volume and its effects on reactive gas uptake. *J Appl Physiol* 1991, 70:2193-2205
23. Plopper CG, Chow CK, Dungworth DL, Brummer M, Nemeth TJ: Effect of low level of ozone on rat lungs. II. morphological responses during recovery and re-exposure. *Exp Mol Pathol* 1979, 29:400-411
24. Johnson DA, Winters RS, Lee KR, Smith CE: Oxidant effects on rat and human lung proteinase inhibitors. *HEI* 1990; Rep. No. 37:1-39